AFRL-VA-WP-TP-2006-348

FEEDBACK CONTROL FOR AERODYNAMICS (PREPRINT)

R. Chris Camphouse, Seddik M. Djouadi, and James H. Myatt

SEPTEMBER 2006

Approved for public release; distribution is unlimited.

STINFO COPY

AIR VEHICLES DIRECTORATE
AIR FORCE MATERIEL COMMAND
AIR FORCE RESEARCH LABORATORY
WRIGHT-PATTERSON AIR FORCE BASE, OH 45433-7542

REPORT DOCUMENTATION PAGE

Form Approved
OMB No. 0704-0188

1. REPORT DATE *(DD-MM-YY)*	2. REPORT TYPE	3. DATES COVERED *(From - To)*
September 2006	Conference Paper Preprint	10/01/2005 – 09/30/2006

4. TITLE AND SUBTITLE

BASIS CONSTRUCTION FOR THE DESIGN OF BOUNDARY FEEDBACK CONTROLS FROM REDUCED ORDER MODELS (PREPRINT)

5a. CONTRACT NUMBER
In-house

5b. GRANT NUMBER

5c. PROGRAM ELEMENT NUMBER
0601102F

6. AUTHOR(S)

R. Chris Camphouse and James H. Myatt (AFRL/VACA)
Seddik M. Djouadi (The University of Tennessee)

5d. PROJECT NUMBER
A03D

5e. TASK NUMBER

5f. WORK UNIT NUMBER
0B

7. PERFORMING ORGANIZATION NAME(S) AND ADDRESS(ES)

Control Design and Analysis Branch (AFRL/VACA)
Control Sciences Division
Air Vehicles Directorate
Air Force Materiel Command, Air Force Research Laboratory
Wright-Patterson Air Force Base, OH 45433-7542

The University of Tennessee
Department of Electrical and Computer Engineering
Knoxville, TN

8. PERFORMING ORGANIZATION REPORT NUMBER
AFRL-VA-WP-TP-2006-348

9. SPONSORING/MONITORING AGENCY NAME(S) AND ADDRESS(ES)

Air Vehicles Directorate
Air Force Research Laboratory
Air Force Materiel Command
Wright-Patterson Air Force Base, OH 45433-7542

10. SPONSORING/MONITORING AGENCY ACRONYM(S)
AFRL-VA-WP

11. SPONSORING/MONITORING AGENCY REPORT NUMBER(S)
AFRL-VA-WP-TP-2006-348

12. DISTRIBUTION/AVAILABILITY STATEMENT
Approved for public release; distribution is unlimited.

13. SUPPLEMENTARY NOTES
Conference paper submitted to the Proceedings of the 2006 45th IEEE Conference on Decision and Control (CDC), published by IEEE.

 PAO Case Number: AFRL/WS 06-2768 (cleared November 29, 2006). Paper contains color.

14. ABSTRACT

The two-dimensional Burgers equation is used as a surrogate for the governing equations to test order-reduction and control design approaches. This scalar equation is selected because it has a nonlinearity that is similar to the Navier-Stokes equation, but it can be accurately simulated using far fewer states. However, the number of states required is still well above that for which a controller can be designed directly. Two approaches for order reduction are used. In both approaches, proper orthogonal decomposition (POD), also know as Karhunen-Loève decomposition or principal component analysis, is used with Galerkin projection. In the first method, the traditional POD approach of selecting the modes to be retained in the reduced-order model is based on the energy content of the modes. In the second method, balanced truncation is used to select the appropriate modes. Both approaches capture the dynamics of the input-output system and are used for control design.

15. SUBJECT TERMS
flow control, Burgers' equation, aerodynamics, fluid mechanics

16. SECURITY CLASSIFICATION OF:			17. LIMITATION OF ABSTRACT:	18. NUMBER OF PAGES	19a. NAME OF RESPONSIBLE PERSON (Monitor)
a. REPORT	b. ABSTRACT	c. THIS PAGE			James H. Myatt
Unclassified	Unclassified	Unclassified	SAR	18	19b. TELEPHONE NUMBER *(Include Area Code)* N/A

Standard Form 298 (Rev. 8-98)
Prescribed by ANSI Std. Z39-18

Feedback Control for Aerodynamics

R. Chris Camphouse,* Seddik M. Djouadi †, and James H. Myatt ‡

1. Abstract

The two-dimensional Burgers equation is used as a surrogate for the governing equations to test order-reduction and control design approaches. This scalar equation is selected because it has a nonlinearity that is similar to the Navier-Stokes equation, but it can be accurately simulated using far fewer states. However, the number of states required is still well above that for which a controller can be designed directly. Two approaches for order reduction are used. In both approaches, proper orthogonal decomposition (POD), also know as Karhunen-Loève decomposition or principal component analysis, is used with Galerkin projection. In the first method, the traditional POD approach of selecting the modes to be retained in the reduced-order model is based on the energy content of the modes. In the second method, balanced truncation is used to select the appropriate modes. Both approaches capture the dynamics of the input-output system and are used for control design.

2. Introduction

Aerodynamic flow control is a research area of great interest to the United States Air Force and the fluid mechanics community in general. Recent advances in actuators, sensors, simulation, and experimental diagnostics bring applications such as suppression of acoustic tones in cavities, separation control for high lift, and trajectory control without moving hinged surfaces within reach. However, many applications require the integration of feedback control because of the need for robustness to flight condition and vehicle attitude, precision tracking, overcoming low-fidelity models, or moving a system away from a stable solution or limit cycle as efficiently as possible. Feedback control strategies in which the bandwidth of the controller is commensurate with the time scales of the aerodynamics are attractive because they offer the possibility of improved performance and reduced control power required through control of unstable structures in the flow field. Unfortunately, models that capture the relevant dynamics of the input-output system and are amenable to control design are difficult to develop.

The governing equations for a compressible fluid are partial differential equations - 1) the Navier-Stokes equation for momentum, 2) the continuity equation, and 3) the energy equation. As an illustration of the complexity of the governing equations, the dimensionless Navier-Stokes equation for momentum [1] for an incompressible, Newtonian fluid with a few simplifying assumptions such as no body force is

$$\frac{\partial \vec{u}}{\partial t} + (\vec{u} \cdot \nabla)\vec{u} + \nabla p = \frac{1}{Re}\Delta \vec{u}, \tag{1}$$

where $\vec{u} = \vec{u}(t,x,y,z)$ is the velocity, $p = p(t,x,y,z)$ is the pressure, and the dimensionless Reynolds number Re is a measure of the ratio of inertia forces to viscous forces. As Re increases with vehicle size and speed, the effect of the linear terms is diminished and the nonlinear terms become more dominant. This greatly increases challenges of both the modeling and control problems for vehicles at realistic flight conditions.

Computational fluid dynamics (CFD) simulations can provide solutions to a discretized form of the Navier-Stokes. However, accurate simulations for simple shapes such as two-dimensional airfoils can require several thousand states and therefore are not directly useful for control design due to the extremely high order of the system. Simulations for a full vehicle can require over one million states. The large number of states is necessary to capture important flow features that occur at extremely small spatial scales. Another challenge for designing control laws for flow control is that the Navier-Stokes equations in traditional form are not affine. Therefore, it is necessary to separate the portions of the discretized system where the control input enters the system for control design. In addition, the location of the actuator is often limited to the boundary. This eliminates the possibility of full-state feedback.

 R. Camphouse is with the U.S. Air Force Research Laboratory, Wright-Patterson Air Force Base, Ohio 45433 russell.camphouse@wpafb.af.mil

†S. Djouadi is with the Department of Electrical and Computer Engineering at The University of Tennessee, Knoxville djouadi@ece.utk.edu

‡J. Myatt is with the U.S. Air Force Research Laboratory, Wright-Patterson Air Force Base, Ohio 45433 james.myatt@wpafb.af.mil

3. Model Problem

3.1. Motivation: Boundary Feedback Control

Reduced order modelling has received significant attention by the research community in recent years. Proper orthogonal decomposition (POD) has been investigated extensively [2]-[10] as a potential technique due to its significant order reduction capability. Full order system model behavior described by thousands of states can often be captured with a POD model composed of dozens of states or less. The implications for control law design are obvious. Applications requiring exceedingly large systems for accurate simulation result in intractable feedback control problems. A particular example is feedback control of aerodynamic fluid flows. Accurate simulations done with computational fluid dynamics typically require discretized flow models describing thousands of states, usually millions in the case of three-dimensional turbulent flow. The systematic development of feedback control laws from systems of such large dimension is currently an intractable problem. Reduction of system order must be done if feedback control law design for these systems is to be feasible.

In many practical applications, boundary actuation is a requirement. For example, control of flow separation over an airfoil requires that actuation and sensing be done on the airfoil surface. The possibility of unmodelled dynamics in the system, or dynamics lost in the order reduction process, make feedback control a requirement. Systematic development of boundary feedback control laws from POD models has remained an elusive problem. Controls are often included in the reduced model in an ad-hoc way, specified to be distributed over a subregion of the domain interior, or simply specified through open-loop forcing.

In this paper, we utilize the weak formulation of reduced order models obtained via POD and Galerkin projection. Use of the weak form permits separation of the boundary input in the reduced model, allowing the boundary control to enter the reduced model equations explicitly. We present these concepts using a nonlinear convective system defined over an obstacle geometry. The resulting model problem captures many of the difficulties associated with feedback control of fluid flows with a greatly reduced computational workload.

3.2. Distributed Parameter System

Let $\Omega_1 \subseteq \mathbb{R}^2$ be the rectangle given by $(a,b]\times(c,d)$. Let $\Omega_2 \subseteq \Omega_1$ be the rectangle given by $[a_1,a_2]\times[b_1,b_2]$ where $a<a_1<a_2<b$ and $c<b_1<b_2<d$. The problem domain, Ω, is given by $\Omega = \Omega_1 \setminus \Omega_2$. In this configuration, Ω_2 is the obstacle. Dirichlet boundary controls are located on the obstacle bottom and top, denoted by Γ_B and Γ_T, respectively.

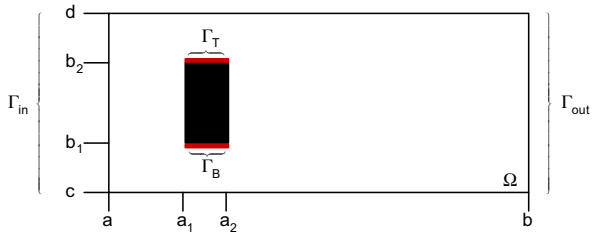

Figure 1. Problem Geometry.

The dynamics of the system are described by the two-dimensional Burgers equation

$$\frac{\partial}{\partial t}w(t,x,y) + \nabla \cdot F(w) = \frac{1}{Re}\Delta w(t,x,y) \tag{2}$$

for $t>0$ and $(x,y)\in\Omega$. In (2), $F(w)$ has the form

$$F(w) = \left[C_1\frac{w^2(t,x,y)}{2} \qquad C_2\frac{w^2(t,x,y)}{2}\right]^T, \tag{3}$$

where C_1, C_2 are nonnegative constants. This system has a convective nonlinearity like that found in the Navier-Stokes partial differential equations modeling fluid flows. The quantity Re, a nonnegative constant, is analogous to the Reynolds number in the Navier-Stokes equations.

To complete the model of the system, boundary conditions must be specified as well as an initial condition. For simplicity, boundary controls are assumed to be separable. With this assumption, we specify conditions on the obstacle bottom and top of the form

$$w(t,\Gamma_B) = u_B(t)\Psi_B(x), \tag{4}$$
$$w(t,\Gamma_T) = u_T(t)\Psi_T(x). \tag{5}$$

In (4)-(5), $u_B(t)$ and $u_T(t)$ are the controls on the bottom and top of the obstacle, respectively. The profile functions $\Psi_B(x)$ and $\Psi_T(x)$ describe the spatial influence of the controls on the boundary. A parabolic inflow condition is specified of the form

$$w(t,\Gamma_{in}) = f(y). \tag{6}$$

At the outflow, a Neumann condition is specified according to

$$\frac{\partial}{\partial x}w(t,\Gamma_{out}) = 0. \tag{7}$$

For notational convenience, denote the remaining boundary as Γ_U. We require that values be fixed at zero along Γ_U as time evolves. The resulting boundary condition is of the form

$$w(t,\Gamma_U) = 0. \tag{8}$$

The initial condition of the system is given by

$$w(0,x,y) = w_0(x,y) \in L^2(\Omega). \tag{9}$$

3.3. POD Basis Construction

The snapshot method [11] is used to construct a low order POD basis for the distributed parameter system. An ensemble of solution snapshots $\{S_i(\mathbf{x})\}_{i=1}^{N}$ for system (2), (4)-(9) is generated by numerical simulation. In (3), we set $C_1 = 1$ and $C_2 = 0$ in order to obtain solutions that convect from left to right for positive inflow condition $f(y)$. In addition, we specify that $Re = 300$. Finite-difference spatial discretization is done as in [12]. A uniform Cartesian grid is constructed with spatial step-size h. The resulting discretized system describes roughly 2,000 states. As it is desired that the POD basis spans dynamics introduced by a time-varying boundary control input, nontrivial boundary conditions are specified during ensemble generation. Inputs specified are of the form

$$u_B(t) = Dsin(0.25t^{2.25}) \qquad u_T(t) = 0, \tag{10}$$

$$u_B(t) = 0 \qquad u_T(t) = Dsin(0.25t^{2.25}), \tag{11}$$

for $D = -3$, -2, -1. The steady solution arising from a positive parabolic inflow condition is taken as the initial condition in each simulation. For each case of control input listed in (10) - (11), snapshots are taken in increments of $\Delta t = 0.1$ starting from $t = 0$ and ending at $T = 15$. The snapshots resulting from each case are combined into an overall snapshot set. The resulting ensemble consists of roughly 900 snapshots.

With the snapshot ensemble in hand, the $N \times N$ correlation matrix L defined by

$$L_{i,j} = \langle S_i, S_j \rangle \tag{12}$$

is constructed. In this work, we utilize the standard $L^2(\Omega)$ inner product

$$\langle S_i, S_j \rangle = \int_\Omega S_i S_j^* \mathbf{dx}, \tag{13}$$

where S_j^* denotes the complex conjugate of S_j, in the construction of L.

With M denoting the number of POD modes to be constructed, the first M eigenvalues of largest magnitude, $\{\lambda_i\}_{i=1}^{M}$, of L are found. They are sorted in descending order, and their corresponding eigenvectors $\{v_i\}_{i=1}^{M}$ are calculated. Each eigenvector is normalized so that

$$\|v_i\|^2 = \frac{1}{\lambda_i}. \tag{14}$$

The orthonormal POD basis set $\{\phi_i(\mathbf{x})\}_{i=1}^{M}$ is constructed according to

$$\phi_i(\mathbf{x}) = \sum_{j=1}^{N} v_{i,j} S_j(\mathbf{x}), \tag{15}$$

where $v_{i,j}$ is the j^{th} component of v_i.

With a POD basis in hand, the solution $w(t,\mathbf{x})$ of the distributed parameter model is approximated as a linear combination of POD modes, i.e.,

$$w(t,\mathbf{x}) \approx \sum_{i=1}^{M} \alpha_i(t)\phi_i(\mathbf{x}). \tag{16}$$

3.4. Weak Galerkin Model

We now develop a reduced order model for the system described by (2), (4)-(9). Using the weak formulation of the governing equation allows us to extract boundary condition information prior to Galerkin projection. Galerkin projection of the weak system onto the POD basis results in a system of ordinary differential equations for the temporal coefficients $\{\alpha_i\}_{i=1}^{M}$ with explicit control input.

Taking the inner product of both sides of (2) with the i-th POD mode $\phi_i(x,y)$ and utilizing Green's identities results in the weak formulation

$$\begin{aligned}
&\int_\Omega \frac{\partial}{\partial t} w(t,x,y)\phi_i(x,y)\mathbf{dx} = \\
&\int_\Omega F \cdot \nabla\phi_i(x,y)\mathbf{dx} - \int_{\partial\Omega} (F(w)\cdot\mathbf{n})\phi_i(x,y)dA(\mathbf{x}) \\
&\qquad + \frac{1}{Re}\left[\int_{\partial\Omega} (\nabla w(t,x,y)\cdot\mathbf{n})\phi_i(x,y)dA(\mathbf{x})\right] \\
&\qquad\qquad - \frac{1}{Re}\left[\int_\Omega \nabla w(t,x,y)\cdot\nabla\phi_i(x,y)\mathbf{dx}\right],
\end{aligned} \tag{17}$$

where $\mathbf{n}$ denotes the unit outward normal.

As seen in (15), each POD mode is a linear combination of solution snapshots. From (8), snapshot values along Γ_U are specified to be zero. As a result, POD modes are zero along Γ_U. Thus, the second boundary integral in (17) is decomposed as

$$\begin{aligned}
&\int_{\partial\Omega} (\nabla w(t,x,y)\cdot\mathbf{n})\phi_i(x,y)dA(\mathbf{x}) = \\
&\int_{a_1}^{a_2} \left(\frac{\partial}{\partial y} w(t,x,b_1)\phi_i(x,b_1) - \frac{\partial}{\partial y} w(t,x,b_2)\phi_i(x,b_2)\right) dx \\
&\qquad\qquad - \int_c^d \frac{\partial}{\partial x} w(t,a,y)\phi_i(a,y)dy,
\end{aligned} \tag{18}$$

where condition (7) has been used to specify that

$$\int_c^d \frac{\partial}{\partial x} w(t,b,y)\phi_i(b,y)dy = 0. \tag{19}$$

In a similar fashion, the remaining boundary integral in (17) is decomposed as

$$\begin{aligned}
&\int_{\partial\Omega} (F(w)\cdot\mathbf{n})\phi_i(x,y)dA(\mathbf{x}) = \\
&\qquad \frac{1}{2}\int_c^d \left(w(t,b,y)^2\phi_i(b,y) - f(y)^2\phi_i(a,y)\right) dy,
\end{aligned} \tag{20}$$

where (6) has been used to incorporate the inflow condition $f(y)$.

Control inputs and the Dirichlet inflow condition are not explicit in (18). They can be made explicit by approximating partial derivatives along the boundary. For $h > 0$, we see that

$$\frac{\partial}{\partial y}w(t,x,b_1) \approx \frac{u_B(t)\Psi_B(x) - w(t,x,b_1-h)}{h}, \quad (21)$$

$$\frac{\partial}{\partial y}w(t,x,b_2) \approx \frac{w(t,x,b_2+h) - u_T(t)\Psi_T(x)}{h}, \quad (22)$$

$$\frac{\partial}{\partial x}w(t,a,y) \approx \frac{w(t,a+h,y) - f(y)}{h}. \quad (23)$$

These expressions are substituted into (18). Approximating $w(t,x,y)$ as a linear combination of POD modes in (17), (18), and (20) results in a reduced order system model. By defining μ as

$$\mu = \frac{1}{hRe}, \quad (24)$$

the reduced order model is of the form

$$\dot{\alpha} = A\alpha + Bu + N(\alpha) + F, \quad (25)$$

where

$$A(i,j) = -\mu[\int_{a_1}^{a_2}(\phi_j(x,b_1-h)\phi_i(x,b_1) + \phi_j(x,b_2+h)\phi_i(x,b_2))dx + \int_c^d \phi_j(a+h,y)\phi_i(a,y)dy + h\int_\Omega \nabla\phi_i(x,y)\cdot\nabla\phi_j(x,y)]\mathbf{dx}, \quad (26)$$

$$B = \mu\begin{bmatrix} \int_{a_1}^{a_2}\phi_1(x,b_1)\Psi_B(x)dx & \int_{a_1}^{a_2}\phi_1(x,b_2)\Psi_T(x)dx \\ \vdots & \vdots \\ \int_{a_1}^{a_2}\phi_M(x,b_1)\Psi_B(x)dx & \int_{a_1}^{a_2}\phi_M(x,b_2)\Psi_T(x)dx \end{bmatrix}_{M\times 2}, \quad (27)$$

$$N(\alpha) = \frac{1}{2}\begin{bmatrix} \int_\Omega\left(\sum_{j=1}^M \alpha_j\phi_j(x,y)\right)^2 \frac{\partial}{\partial x}\phi_1(x,y)\mathbf{dx} \\ \vdots \\ \int_\Omega\left(\sum_{j=1}^M \alpha_j\phi_j(x,y)\right)^2 \frac{\partial}{\partial x}\phi_M(x,y)\mathbf{dx} \end{bmatrix}_{M\times 1} - \frac{1}{2}\begin{bmatrix} \int_c^d\left(\sum_{j=1}^M \alpha_j\phi_j(b,y)\right)^2 \phi_1(b,y)dy \\ \vdots \\ \int_c^d\left(\sum_{j=1}^M \alpha_j\phi_j(b,y)\right)^2 \phi_M(b,y)dy \end{bmatrix}_{M\times 1}, \quad (28)$$

$$F = \begin{bmatrix} \int_c^d(\mu f(y) + \frac{1}{2}f(y)^2)\phi_1(a,y)dy \\ \vdots \\ \int_c^d(\mu f(y) + \frac{1}{2}f(y)^2)\phi_M(a,y)dy \end{bmatrix}_{M\times 1}. \quad (29)$$

Projecting the initial condition $w_0(x,y)$ onto the POD basis results in an initial condition for the reduced order model of the form

$$\alpha(0) = \alpha_0. \quad (30)$$

3.5. Model Validation

Before using the reduced order model in (25) to design feedback control laws, we first verify agreement between the reduced and full order systems. We utilize the ratio

$$100\left(\frac{\sum_{i=1}^M \lambda_i}{\sum_{i=1}^N \lambda_i}\right) \quad (31)$$

to determine how many POD modes to include in the reduced model. The POD basis is optimal in an energy sense [13]. It captures the mean square energy of the snapshot ensemble better than any other basis. The quantity in (31) provides a measure of the ensemble energy that is captured by the POD basis. By requiring that 99.9% of the energy contained in the snapshot ensemble be contained in the POD basis, we calculate the smallest value of M such that the quantity in (31) is greater than or equal to 99.9. For our snapshot ensemble, the smallest value of M satisfying this relationship is 15. Thus, we include 15 POD modes in the construction of the reduced model in (25). The first nine modes are shown in Figure 2.

We now compare the solution obtained from the reduced and full order models using different boundary inputs that those used during ensemble creation. Boundary

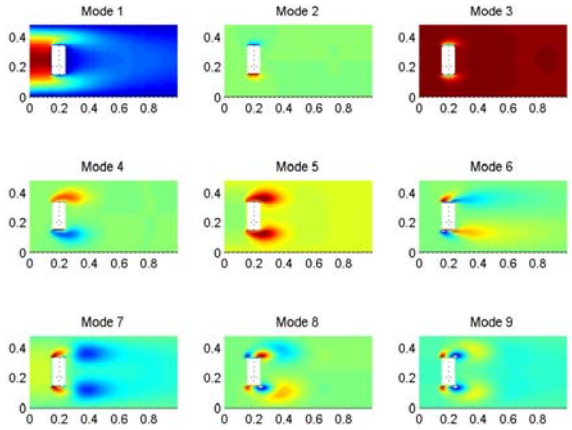

Figure 2. 9 POD Modes.

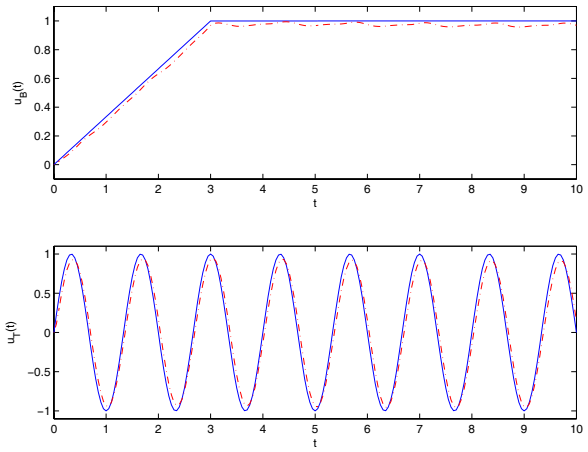

Figure 3. Boundary Condition Accuracy.

inputs specified are of the form

$$u_B(t) = min\left(\frac{t}{3}, 1\right), \tag{32}$$

$$u_T(t) = sin\left(\frac{3}{2}\pi t\right). \tag{33}$$

We first verify boundary condition agreement between the full order system and the linear combination of POD modes given by (16) with the modes restricted to the boundary. By specifying characteristic functions for the control profile functions $\Psi_B(x)$ and $\Psi_T(x)$ in (4)-(5), we see that

$$\sum_{i=1}^{M} \alpha_i(t)\phi_i(\Gamma_B) \approx w(t,\Gamma_B) = u_B(t), \tag{34}$$

$$\sum_{i=1}^{M} \alpha_i(t)\phi_i(\Gamma_T) \approx w(t,\Gamma_T) = u_T(t), \tag{35}$$

We construct the linear combinations given on the left of (34)-(35) and compare them to the boundary inputs given by (32)-(33). The results are shown in Figure 3. In Figure 3, dashed lines denote the linear combination of POD modes restricted to the boundary. Solid lines denote the boundary inputs defined by (32)-(33). As can be seen in Figure 3, there is very good agreement between the boundary conditions specified for the full order system and the linear combination of POD modes restricted to the boundary. To further validate the reduced model, we project the solution from the full order simulation at each time step onto the POD basis. The resulting temporal coefficients are compared to those predicted from the reduced order model. The results obtained for the first five temporal coefficients are shown in Figure 4. In that figure, solid curves denote values of temporal coefficients obtained from the projection. Dashed curves denote the solution of the reduced order model. As seen in Figure 4, very good agreement is

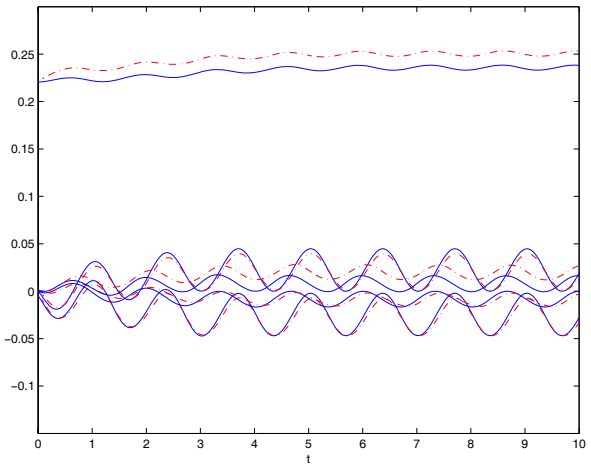

Figure 4. Projected And POD Model Coefficients.

seen between the full and reduced solutions even though the open-loop input considered was not specifically incorporated in the snapshot ensemble.

3.6. Linear Quadratic Control

The system given by (25), (30) is linearized about the origin yielding a state-space equation of the form

$$\dot{\alpha}(t) = A\alpha + Bu, \tag{36}$$

$$\alpha(0) = \alpha_0. \tag{37}$$

We consider the tracking problem for (36)-(37). A fixed reference signal $w_{ref}(\mathbf{x})$ is specified for the full order system. Projecting $w_{ref}(\mathbf{x})$ onto the POD basis yields tracking coefficients for the reduced order model, denoted by α_{ref}.

The dynamics of the linearized model under tracking control are given by

$$\begin{bmatrix} \dot{\alpha} \\ \alpha_{ref} \end{bmatrix} = \begin{bmatrix} A & 0 \\ 0 & 0 \end{bmatrix} \begin{bmatrix} \alpha \\ \alpha_{ref} \end{bmatrix} + \begin{bmatrix} B \\ 0 \end{bmatrix} u \tag{38}$$

$$= \bar{A}X + \bar{B}u, \tag{39}$$

where we have defined the augmented state X as

$$X(t) = \begin{bmatrix} \alpha(t) \\ \alpha_{ref} \end{bmatrix} \text{ with } X_0 = \begin{bmatrix} \alpha_0 \\ \alpha_{ref} \end{bmatrix}. \tag{40}$$

To formulate the control problem, we consider the γ-shifted linear quadratic regulator (LQR) cost function

$$J(\alpha_0, u) = \int_0^\infty \left\{ (\alpha - \alpha_{ref})^T Q(\alpha - \alpha_{ref}) + u^T R u \right\} e^{2\gamma t} dt. \tag{41}$$

In (41), Q is a diagonal, symmetric, positive semi-definite matrix of state weights. R is a diagonal, symmetric, positive definite matrix of control weights. The quantity γ, a nonnegative constant, is an additional parameter that provides added robustness in the control [15]. The optimal control problem we consider is to minimize (41) over all controls $u \in L^2(0,\infty)$ subject to the constraints (38)-(40).

For a controllable system, the LQR problem has a unique solution of the form

$$u_{opt} = -KX \tag{42}$$

$$= -[K_1 \quad K_2]X \tag{43}$$

$$= -\left[R^{-1}B^T\Pi_{11} \quad R^{-1}B^T\Pi_{12}\right]X, \tag{44}$$

where Π_{11} is the unique symmetric, non-negative solution of the algebraic Riccati equation

$$(A+\gamma I)^T\Pi_{11} + \Pi_{11}(A+\gamma I) - \Pi_{11}BR^{-1}B^T\Pi_{11} + Q = 0. \tag{45}$$

The matrix Π_{12} in (44) satisfies the equation

$$\left[(A+\gamma I)^T - \Pi_{11}BR^{-1}B^T\right]\Pi_{12} = Q. \tag{46}$$

The feedback control obtained from the linearized model is placed into the nonlinear state-space equation. As discussed in [14]-[15], the resulting closed-loop nonlinear system is of the form

$$\dot{X} = (\bar{A} - \bar{B}K)X + [N(\alpha)\ 0]^T + [F\ 0]^T, \tag{47}$$

$$X(0) = X_0. \tag{48}$$

3.7. Closed-Loop Results

The tracking LQR problem requires the specification of the reference signal $w_{ref}(\mathbf{x})$. In the results that follow, $w_{ref}(\mathbf{x})$ is defined as the unactuated steady solution for the case $Re = 50$. To obtain the reference function for the reduced model, we project $w_{ref}(\mathbf{x})$ onto the fifteen POD modes. The values obtained are used as tracking coefficients in the reduced order control problem. The reference signal obtained by projecting $w_{ref}(\mathbf{x})$ onto the POD basis is shown in Figure 5.

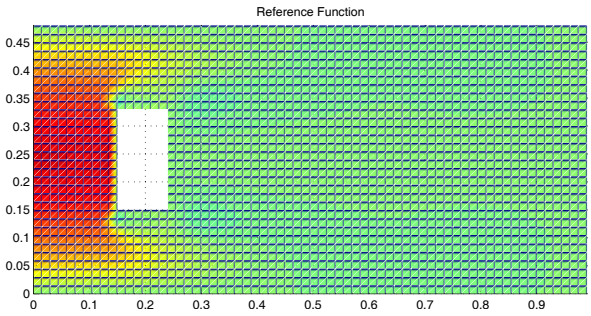

Figure 5. Reference Signal.

The values specified in the control formulation are $Q = 3500I^{15\times15}$, $R = I^{2\times2}$, and $\gamma = 0.41$. We specify $w_0(x)$ to be the steady-state solution for the case of $Re = 300$. Therefore, the solution will remain at $w_0(x)$ until the boundary condition at the actuator location is altered by the controller. The controlled reduced order model is shown in Figure 6. By comparing the controlled solution of Figure 6 to the reference function in Figure 5, it is apparent that the reduced order control satisfies the control objective quite well. Significant tracking is achieved.

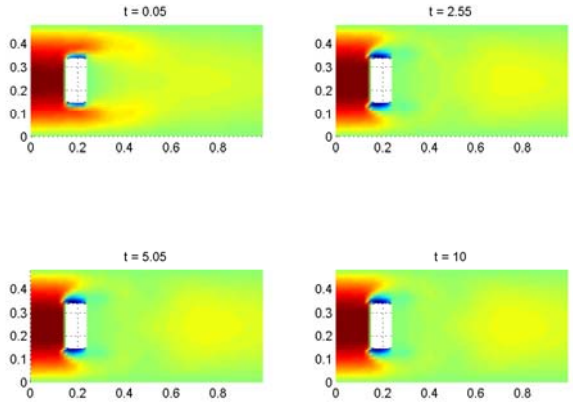

Figure 6. Controlled POD Model.

4. Balanced Truncation and H$^\infty$ Control

4.1. Balanced Truncation

Balanced truncation is a simple and popular model reduction technique, which can be described as follows [20, 21, 22, 23]: Suppose we have a stable linear time invariant (LTI) system described by the following n-dimensional state space equation

$$\begin{aligned} \dot{x}(t) &= Ax(t)+Bu(t) \\ y(t) &= Cx(t) \end{aligned} \tag{49}$$

where $x(t)$ is the $n\times 1$-state vector of the system, $u(t)$ is an $m\times 1$-input vector, and $y(t)$ is an $p\times 1$-output or measurement vector. A, B, and C are constant matrices of appropriate dimensions.

The underlying idea of balanced truncation is to take into account both the input and output signals of the system when deciding which states to truncate with appropriate scaling. The latter is performed by transforming the controllability and observability gramians, denoted W_c and W_o respectively, so that they are equal and diagonal.

The controllability and observability gramians satisfy the following Lypaunov equations [21]

$$AW_c + W_cA^T + BB^T = 0 \tag{50}$$

$$A^TW_o + W_oA + C^TC = 0 \tag{51}$$

The controllability and observability gramians can be represented as

$$\begin{aligned} W_c &= \int_0^\infty e^{At}BB^Te^{A^Tt}dt \\ W_o &= \int_0^\infty e^{A^Tt}C^TCe^{At}dt \end{aligned} \tag{52}$$

Computing a state balancing transformation M is achieved by first calculating the matrix [21, 22]

$$W_{co} = W_cW_o \tag{53}$$

and determining its eigenmodes

$$W_{co} = M\Lambda M^{-1} \tag{54}$$

Let

$$z(t) := M^{-1}x(t) \tag{55}$$

then the resulting transformed state space is

$$\begin{aligned} \dot{z}(t) &= \tilde{A}z(t)+\tilde{B}u(t) \\ y(t) &= \tilde{C}z(t) \end{aligned} \tag{56}$$

where

$$\begin{aligned} \tilde{A} &:= M^{-1}AM \\ \tilde{B} &:= M^{-1}B \\ \tilde{C} &:= CM \end{aligned}$$

The transformation M is chosen such that the controllability and observability gramians for the transformed system satisfy

$$\tilde{W}_c = \tilde{W}_o = M^{-1}W_cM^{-1T} = M^TW_oM =: \Sigma \tag{57}$$

where Σ is a diagonal matrix that satisfies $\Sigma^2 = \Lambda$, and the diagonal elements of Σ, σ_i's, are known as the Hankel singular vales of the system, i.e.,

$$\Sigma = \mathrm{diag}\{\sigma_1,\ \sigma_2,\ \cdots,\ \sigma_n\} \tag{58}$$

where σ_i are the Hankel singular values of the system G arranged in non-increasing order

$$\sigma_1 \geq \sigma_2 \geq \cdots \geq \sigma_n \geq 0 \tag{59}$$

In balanced truncation only states corresponding to large Hankel singular values are retained. Small Hankel singular values correspond to states which are deemed weakly controllable and weakly observable, and therefore deleted from the state-space model. For instance, if the first n_r states are retained then the resulting transformation is given by

$$M_r = [I_r \quad 0]M \tag{60}$$

where I_r is the $n_r\times n_r$ identity matrix. The reduced order model is obtained by letting

$$x_r = [I_r \quad 0]Mx \tag{61}$$

as follows

$$\begin{aligned} \dot{x}_r(t) &= [I_r \quad 0]M^{-1}AM\begin{bmatrix} I_r \\ 0 \end{bmatrix}x_r(t) + [I_r \quad 0]M^{-1}Bu(t) \\ y_r(t) &= CM\begin{bmatrix} I_r \\ 0 \end{bmatrix}x_r(t) \end{aligned} \tag{62}$$

Let

$$\begin{aligned} A_r &:= [I_r \quad 0]M^{-1}AM\begin{bmatrix} I_r \\ 0 \end{bmatrix} \\ B_r &:= [I_r \quad 0]M^{-1}B \\ C_r &:= CM\begin{bmatrix} I_r \\ 0 \end{bmatrix} \end{aligned} \tag{63}$$

The error bound for the output is given by

$$\|y(t)-y_r(t)\|_2 \leq 2\sum_{n_r+1}^{n}\sigma_i\|u(t)\|_2, \quad \forall u\in L^2 \tag{64}$$

Balanced truncation is optimal in a precise sense [26]. To see this define a causal bounded input-output operator G acting on $L^2(-\infty,\,\infty)$ into $L^2(-\infty,\,\infty)$ described by the convolution [22, 23]

$$(Gu)(t) := \int_{-\infty}^{t} Ce^{A(t-\tau)}Bu(\tau)d\tau \tag{65}$$

Now, define the Hankel operator

$$\Gamma_G :\; L^2(-\infty,\,0] \longmapsto L^2[0,\,\infty)$$

of G by

$$\Gamma_G := P_+ G|_{L^2(-\infty,\,0]} \tag{66}$$

where $G\big|_{L^2(-\infty,\,0]}$ denotes the restriction of G to $L^2(-\infty,\,0]$, and P_+ is the orthogonal projection acting from $L^2(-\infty,\,\infty)$ into $L^2[0,\,\infty)$, i.e., P_+ is the truncation operator

$$P_+ f(t) = \left\{ \begin{array}{ll} f(t) & \text{if } t \geq 0 \\ 0 & \text{if } t < 0 \end{array} \right. ,\; f(t) \in L^2(-\infty,\,\infty) \tag{67}$$

Then, the Hankel operator Γ_G can be written as

$$\Gamma_G u(t) = \int_{-\infty}^{0} Ce^{A(t-\tau)}Bu(\tau)d\tau, \quad \text{for } t \geq 0 \tag{68}$$

The Hankel operator Γ_G maps past inputs to future outputs. Expression (68) shows that the Hankel operator Γ_G is an integral operator mapping $L^2(-\infty,\,0)$ into $L^2[0,\,\infty)$, with kernel the impulse response $k(t,\,\tau)$ defined by

$$k(t,\,\tau) := Ce^{A(t-\tau)}B, \quad \tau < 0,\; t \geq 0 \tag{69}$$

The Hankel operator Γ_G has finite rank $k \leq n$, that is, its range has finite dimension $k \leq n$ [21, 23], and therefore belongs to the Hilbert-Schmidt class of operators acting from $L^2(-\infty,\,0]$ into $L^2[0,\,\infty)$ [25]. Its Hilbert-Schmidt norm is defined as

$$\|\Gamma_G\|_{\text{HS}}^2 := \int_0^{\infty}\int_{-\infty}^{0} |k(t,\tau)|^2\, d\tau dt \tag{70}$$

Next, consider the optimal distance minimization μ_{n_r} defined in (71), which consists of optimally approximating in the Hilbert-Schmidt norm the Hankel operator Γ_G by another Hankel operator $\Gamma_{G_{n_r}}$ of lesser rank, say $n_r < k$, in other words

$$\mu_{n_r} := \min_{n_r<k} \|\Gamma_G - \Gamma_{G_{n_r}}\|_{\text{HS}} \tag{71}$$

It turns out that the minimizer in (71) is the Hankel operator with kernel the impulse response of the reduced order model (62) [26], i.e.,

$$C_r e^{A_r(t-\tau)}B_r \tag{72}$$

More explicitly [26],

$$\Gamma_{G_{n_r}} u(t) = \int_{-\infty}^{0} C_r e^{A_r(t-\tau)}B_r u(\tau)d\tau, \quad \text{for } t \geq 0 \tag{73}$$

and the optimal index is given by

$$\mu_{n_r} = \|\Gamma_G - \Gamma_{G_{n_r}}\|_{\text{HS}} \tag{74}$$

Optimality of balanced truncation seems to be missing in the literature. In fact, it has been widely claimed that balanced truncation is not optimal in any sense [20, 23, 24].

In terms of kernel approximation, balanced truncation is a particular case of POD in the sense that the kernel we want to approximate is the impulse response of the system $k(t,\,\tau)$ defined in (71). The optimization index μ_{n_r} can then be written as in POD [26]

$$\begin{aligned} \mu_{n_r}^2 &= \min\Big\{\int_0^{\infty}\int_{-\infty}^{0}\Big|k(t,\,\tau) - \sum_{i=1}^{n_r} f_i(t)g_i(\tau)\Big|^2 d\tau dt \\ &\quad : \quad f_i \in L^2[0,\,\infty);\; g_i \in L^2(-\infty,\,0]\Big\} \qquad (75) \\ &= \int_0^{\infty}\int_{-\infty}^{0}\Big|k(t,\,\tau) - C_r e^{A_r(t-\tau)}B_r\Big|^2 d\tau dt \qquad (76) \end{aligned}$$

Expressions (74) and (76) show that balanced truncation is optimal in the sense of optimal approximation in the Hilbert-Schmidt norm of the Hankel operator Γ_G, and optimal in the sense of the $\|\cdot\|_2$-norm of kernels corresponding to impulse responses of linear time-invariant systems defined over $[0,\,\infty)\times(-\infty,\,0]$.

The linear time-invariant system framework allows the exact computations of the optimal lower order model approximation. This contrasts with POD which uses simulation data and particular open-loop inputs to generate snapshots.

4.2. Application to the Weak Galerkin Model

Our approach is to construct an approximately balanced realization to (25). This is carried out by first linearizing (25) around α_0. The state space and output equations have the form

$$\begin{aligned} \dot{\alpha}(t) &= \hat{A}\alpha(t) + \hat{B}u(t), \quad \alpha(0) = \alpha_0 \qquad (77) \\ y(t) &= \alpha(t) \qquad (78) \end{aligned}$$

where $\hat{A}$ is a matrix having the same dimension as A, and is given by

$$\begin{aligned} \hat{A} &= \left.\frac{\partial\big(A\alpha + Bu(t) + N(\alpha) + F\big)}{\partial\alpha}\right|_{\alpha=\alpha_0} \qquad (79) \\ \hat{B} &= \left.\frac{\partial\big(A\alpha + Bu(t) + N(\alpha) + F\big)}{\partial u}\right|_{u} = B \qquad (80) \end{aligned}$$

In this model the dimension of the state vector α is 40 which corresponds to 40 POD modes. A balanced realization is first computed and 27 states truncated, i.e., only the states corresponding to the 13 largest Hankel singular are kept in the model. This results in a 13-dimensional state-space model

$$\begin{aligned} \dot{z}(t) &= \tilde{A}z(t)+\tilde{B}u(t) \\ y(t) &= \tilde{C}z(t) \end{aligned} \tag{81}$$

where $z(t) \in \mathbb{R}^{13}$, $\tilde{B} \in \mathbb{R}^{13\times 2}$, and $C \in \mathbb{R}^{40\times 13}$.

The first 8 POD modes corresponding are shown in Figure 7. We project the solution from the full order

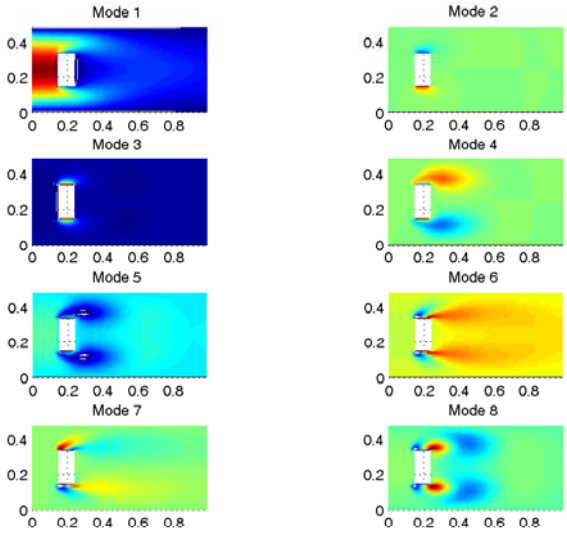

Figure 7. 8 POD Modes.

simulation at each time step onto the POD basis. The resulting first 5 temporal coefficients of the full order model are compared to those predicted from the 13-th order reduced order model output.
In Figure 8, dashed lines denote the linear combination of POD modes restricted to the boundary. Solid lines denote the boundary inputs defined by

$$u_B(t) = \sin\left(\frac{3}{4}\pi t\right) \tag{82}$$

$$u_T(t) = \sin\left(\frac{3}{2}\pi t\right) \tag{83}$$

As can be seen in Figure 8, there is very good agreement between the boundary conditions specified for the full order system and the linear combination of POD modes restricted to the boundary.

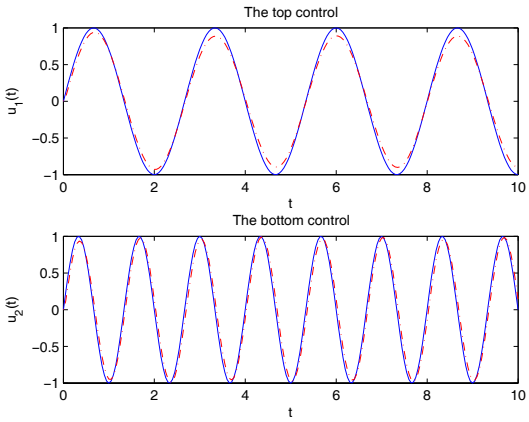

Figure 8. Boundary Condition Accuracy.

The results obtained for the first five temporal coefficients are shown in Figure 9. In that Figure, solid curves denote values of temporal coefficients obtained from the projection. Dashed curves denote the output of the reduced order model. As seen in Figure 9, very good agreement is seen between the full and reduced solutions even though the open-loop input considered was not specifically incorporated in the snapshot ensemble.

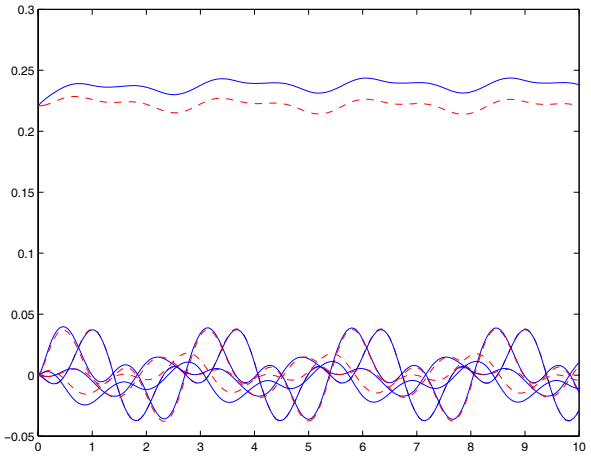

Figure 9. Projected and POD Model Coefficients.

In Figure 10, we compare the full order solution $w(t,\mathbf{x})$ of the Burgers' equation with the solution based on the 13-th order model $w_r(t,\mathbf{x})$, i.e.,

$$w_r(t,\mathbf{x}) = \sum_{i=1}^{40} y_i(t)\phi_i(\mathbf{x}) \tag{84}$$

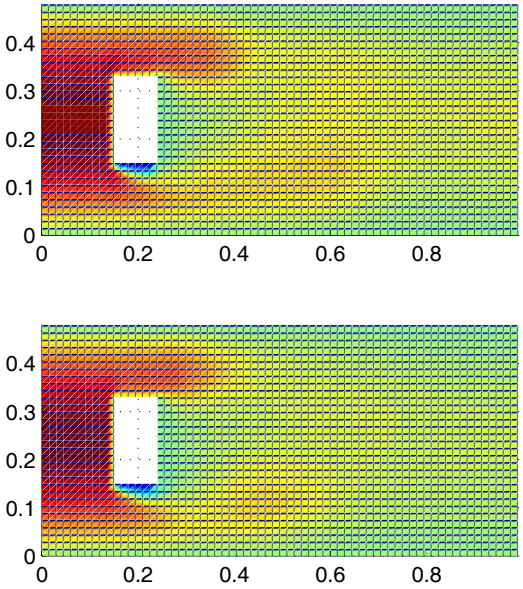

Figure 10. Full and Reduced Order Models' Responses.

Note that despite the fact that only a 13-th order model is used the agreement between the two responses is good.

4.3. H$^\infty$ Control

In this section we consider the design of an H^∞ controller for the tracking problem for (77)-(78). The motivation behind our choice is that H^∞ controllers are robust against unmodeled or neglected dynamics, and unknown or unmeasurable disturbances [21, 22, 23]. As in section 3.6, a fixed reference signal $w_{ref}(\mathbf{x})$ is specified for the full order system. Projecting $w_{ref}(\mathbf{x})$ onto the POD basis yields tracking coefficients for the reduced order model, denoted by α_{ref}. The tracking problem is depicted in Figure 11, where C is the controller and P the plant represented by the dynamical equation (25). The computation of the H^∞ is based on the 13-th order reduced model (81). From Figure 11, for tracking purposes the controlled output is chosen to be the error signal e which is defined to be the difference between the reference α_{ref} and the actual output $y(t)$, i.e.,

$$e(t) := \alpha_{ref} - y(t) \tag{85}$$

The dynamics of the reduced model for tracking control represented in Figure 11 are then given by the state space equation

$$\begin{aligned} \dot{z}(t) &= \tilde{A}z(t) + \tilde{B}_1\alpha_{ref} + \tilde{B}_2u(t) && (86)\\ y(t) &= \tilde{C}z(t) + D_{11}\alpha_{ref} + D_{12}u(t) \\ e(t) &= -\tilde{C}z(t) + D_{21}\alpha_{ref} + D_{22}u(t) && (87) \end{aligned}$$

The objective of the H^∞ controller C is to stabilize the closed-loop system and minimize the effect of α_{ref} on the error e by viewing α_{ref} as an unknown disturbance in L^2 of unit $\|\cdot\|_2$-norm. From Figure 11, in terms of transfer function matrices of P and C, the transfer matrix from α_{ref} to e is given by the sensitivity function $T_{e\alpha_{ref}}$ defined by

$$\begin{aligned} e &= (I+PC)^{-1}\alpha_{ref} && (88)\\ &=: T_{e\alpha_{ref}} && (89) \end{aligned}$$

We compute the worst-case disturbance transmission error

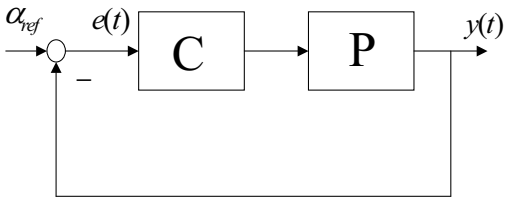

Figure 11. Block Diagram of the Closed-Loop System.

due to α_{ref}, i.e.,

$$\sup_{\|\alpha_{ref}\|_2\le 1} \|e\|_2 \tag{90}$$

which is given by [21, 22, 23]

$$\begin{aligned} \sup_{\|\alpha_{ref}\|_2\le 1} \|e\|_2 &= \operatorname*{ess\,sup}_{0\le\omega<\infty} \sigma\left(T_{e\alpha_{ref}}(j\omega)\right) && (91)\\ &=: \|T_{e\alpha_{ref}}\|_\infty && (92) \end{aligned}$$

where ess sup denotes the essential supremum, and $\sigma(\cdot)$ the maximum singular value of its argument.

The H^∞ control design reduces to the following optimization: Find C such that the closed-loop system is robustly stable and

$$\mu := \min_C \|T_{e\alpha_{ref}}\|_\infty \tag{93}$$

The solution of (93) is textbook material. There are Riccati-based and linear matrix inequalities (LMIs) based techniques to solve (93) [21, 22, 23, 27]. In this work, we

use the LMI approach because of its numerical robustness and stability. The H^∞ problem (93) is directly optimized by solving the following LMI problem [27, 28]:

Minimize γ over $R = R^T$ and $S = S^T$ such that

$$\begin{pmatrix} N_{12} & 0 \\ 0 & I \end{pmatrix}^T \begin{pmatrix} \tilde{A}R + R\tilde{A} & R\tilde{C}^T & \tilde{B}_1 \\ \tilde{C}R & -\gamma I & D_{11} \\ \tilde{B}_1^T & D_{11}^T & -\gamma I \end{pmatrix} \begin{pmatrix} N_{12} & 0 \\ 0 & I \end{pmatrix} < 0$$

$$\begin{pmatrix} N_{21} & 0 \\ 0 & I \end{pmatrix}^T \begin{pmatrix} \tilde{A}S + S\tilde{A} & S\tilde{B}_1 & \tilde{C}^T \\ \tilde{B}_1^T S & -\gamma I & D_{11}^T \\ \tilde{C} & D_{11} & -\gamma I \end{pmatrix} \begin{pmatrix} N_{21} & 0 \\ 0 & I \end{pmatrix} < 0$$

$$\begin{pmatrix} R & I \\ I & S \end{pmatrix} \geq 0$$

where N_{12} and N_{21} denote the bases of the null spaces of $\left(\tilde{B}_2^T,\ D_{12}^T\right)$ and $\left(-\tilde{C},\ D_{21}\right)$, respectively, and I is the identity matrix.

Solving the LMI optimization result in an optimal $\mu = 1$ and an optimal controller C of order 13. Closing the loop on the full order Galerkin model using this controller results in the responses for the temporal coefficients α shown in Figure 12, where we have plotted the first 8 α's. In that Figure, solid curves represent the values of the 8 temporal coefficients α, and dashed lines represent the reference α_{ref}. Note that excellent tracking is achieved with virtually zero steady state error.

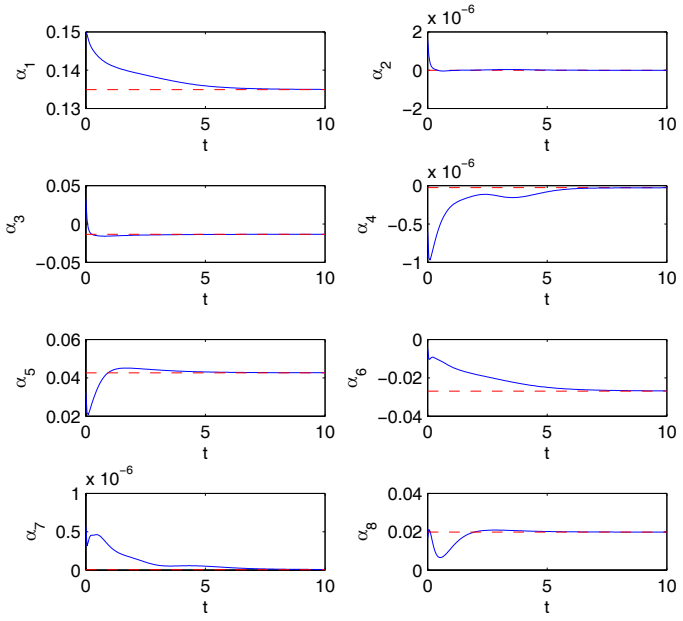

Figure 12. Full Order Closed-Loop System Tracking Response

5. Conclusions

For the two-dimensional Burgers equation, traditional proper orthogonal decomposition and balanced truncation using POD modes are solid approaches for order reduction with the goal of control design. Each method has particular strengths that make it well-suited for this class of problems. Traditional POD maintains nonlinearities and therefore allows the use of the reduced-order model to assess the impact of the nonlinearities on the performance of the controller in reduced-order simulations. It also permits the use of nonlinear control, although that was not a part of the current study. Balanced truncation provides much needed insight into which modes should be maintained in the reduced-order model. Each method also presents challenges. Traditional POD, while providing modes that are physically meaningful, does not always provide modes that are observable or controllable. Balanced truncation requires linearization and is only valid in the vicinity of the equilibrium for which it was developed. Nonetheless, given the success using traditional POD and balanced truncation for the Burgers equation, both methods show promise for use with the Navier-Stokes equations.

6. Future Work

Application of the order-reduction methods will be applied to a two-dimensional, simply-hinged airfoil with multiple synthetic jets in the vicinity of and on the flap to eliminate separation and generate high lift. A well-designed control law is expected to provide the correct phase of the actuators with respect to each other and the flow field dynamics.

References

[1] Aamo, O.M. and Krstić, M., *Flow Control by Feedback: Stabilization and Feedback*, Springer, London, 2003, p. 13.

[2] Atwell, J. and King, B., "Computational Aspects of Reduced Order Feedback Controllers for Spatially Distributed Systems," *Proceedings of the 38th IEEE Conference on Control and Desicion*, December 1999, pp. 4301-4306.

[3] Banks, H., del Rosario, R., and Smith, R., "Reduced Order

Model Feedback Control Design: Numerical Implentation in a Thin Shell Model," Technical Report CRSC-TR98-27, Center for Research in Scientific Computation, North Carolina State University, June, 1998.

[4] Caraballo, E., Samimy, M., and DeBonis, J., "Low Dimensional Modeling of Flow for Closed-Loop Flow Control," AIAA Paper 2003-0059, January 2003.

[5] Carlson, H., Glauser, M., Higuchi, H., and Young, M., "POD Based Experimental Flow Control on a NACA-4412 Airfoil," AIAA Paper 2004-0575, January 2004.

[6] Carlson, H., Glauser, M., and Roveda, R., "Models for Controlling Airfoil Lift and Drag," AIAA Paper 2004-0579, January 2004.

[7] Cohen, K., Siegel, S., McLaughlin, T., and Myatt, J., "Proper Orthogonal Decomposition Modeling of a Controlled Ginzburg-Landau Cylinder Wake Model," AIAA Paper 2003-2405, January 2003.

[8] Efe, M. and Ozbay, H., "Proper Orthogonal Decomposition for Reduced Order Modeling: 2D Heat Flow," *Proc. of 2003 IEEE Conference on Control Applications*, June 23-25, 2003, pp. 1273-1277.

[9] Camphouse, R.C., "Boundary Feedback Control Using Proper Orthogonal Decomposition Models," *Journal of Guidance, Control, and Dynamics*, Vol. 28, No. 5, September-October 2005, pp 931-938.

[10] Camphouse, R. C. and Myatt, J. H., "Reduced Order Modelling and Boundary Feedback Control of Nonlinear Convection," AIAA Paper 2005-5844, August 2005.

[11] Sirovich, L., "Turbulence and the Dynamics of Coherent Structures, Parts I-III," *Quarterly of Applied Mathematics*, Volume 45, Brown University, Rhode Island, 1987, pp. 561-590.

[12] Camphouse, R. and Myatt, J., "Feedback Control for a Two-Dimensional Burgers Equation System Model," AIAA Paper 2004-2411, June 2004.

[13] Holmes, P., Lumley, J., and Berkooz, G., *Turbulence, Coherent Structures, Dynamical Systems and Symmetry*, Cambridge University Press, New York, 1996, pp. 86-127.

[14] Burns, J. and Kang, S., "A Control Problem for Burgers Equation with Bounded Input/Output," *Nonlinear Dynamics*, Volume 2, Kluwer Academic Publishing, New York, 1991, pp. 235-262.

[15] Burns, J. and Kang, S., "A Stabilization Problem for Burgers Equation with Unbounded Control and Observation," *Control and Estimation of Distributed Parameter Systems*, Volume 100, Birkhauser Verlag, Basel, 1991, pp. 51-72.

[16] Bensoussan, A., Prato, G., Delfour, M., and Miller, S., "Representation and Control of Infinite Dimensional Systems," Vol. 2 of *Systems & Control: Foundations & Applications*, Birkhauser, Boston, 1992, pp. 259-317.

[17] Borggaard, J. and Burns, J., "A Continuous Control Design Method," AIAA Paper 2002-2998, June 2002.

[18] Borggaard, J., Burns, J., Zietsman, L., "Computational Challenges in Control of Partial Differential Equations," AIAA Paper 2004-2526, June 2004.

[19] Lasiecka, I. and Triggiani, R., *Control Theory for Partial Differential Equations: Continuous and Approximation Theories Volume 1*, Cambridge University Press, New York, 2000, pp. 178-194.

[20] Moore, B., Principal Component Analysis in Linear Systems: Controllability, Observability, and Model Reduction, *IEEE Transactions on Automatic Control, Vol. AC-26, No. 1, 1981, pp. 17-31.*

[21] K. Zhou, *Essentials of Robust Control*, Prentice-Hall, 1998.

[22] K. Zhou, K. Zhou, J.C. Doyle and K. Glover, *Robust and Optimal Control*, Prentice-Hall, 1996.

[23] G.E. Dullerud and F. Paganini, *A Course in Robust Control Theory*, Springer-Verlag, 2000.

[24] S. Lall, J.E. Marsden and S. Glavas, A subspace approach to balanced truncation for model reduction of nonlinear control systems, Int. J. Robust Nonlinear Control 2002; 12, pp. 519-535.

[25] F. Riesz and B.Sz.-Nagy, *Functional Analysis*, Dover, 1990.

[26] S.M. Djouadi, R.C. Camphouse and J.H. Myatt, Optimality of Proper Orthogonal Decomposition and Balanced Truncation with Application to the Two-Dimensional Burger Equation, in preparation.

[27] R.E. Skelton, T. Iwasaki and K. Grigoriadis, *A Unifie Algebraic Approach to Linear Control Design*, Taylor & Francis, 1998.

[28] P. Gahined, A. Nemirovski, A.J. Laub and M. Chilali, *LMI Control Toolbox*, Taylor & Francis, 1995.